Pseudo-static shakedown analysis of structures using edge-based smoothed finite element method

Phuc L. H. Ho[1], *Dung T. Tran*[2,*]

[1]University Core Research Center for Disaster-free & Safe Ocean City Construction, Dong-A University, Busan 49315, Korea.
[2]Faculty of Civil Engineering, Ho Chi Minh City Open University, Ho Chi Minh City, Vietnam.

*Corresponding Author: Dung T. Tran (email: dung.ttrung@ou.edu.vn)
(Received: 12-January-2024; accepted: 16-April-2024; published: 30-June-2024)
http://dx.doi.org/10.55579/jaec.202482.449

Abstract. *This study introduces a novel numerical procedure for conducting shakedown analysis on structures subjected to cyclic loads. The determination of safety load multipliers is achieved through the integration of the edge-based smoothed finite element method (ES-FEM) and conic programming. By applying the smoothing technique, all constraints are satisfied in an average manner within the smoothing domains, as opposed to at numerous Gauss points in the Finite Element Method (FEM). This approach results in a reduction in the problem size and the number of variables. The formulated optimization problem associated with the standard form of second-order cone programming (SOCP) is addressed using highly efficient solvers. A series of benchmark examples is examined to demonstrate the computational efficacy of the proposed method.*

Keywords: *Shakedown analysis, cyclic loads, SOCP, ES-FEM.*

1. Introduction

Establishing safe limit states is pivotal in engineering structural design. Limit and shakedown analyses, recognized methodologies for estimating collapse loads, play a vital role in supporting safety assessments. In limit analysis, structures undergo incremental loads until reaching a point of load-carrying capacity loss. Conversely, shakedown analysis investigates structures subjected to repeated or cyclic loads. The objective of both analyses is to compute the maximum load that structures can sustain.

Within the framework of limit and shakedown analyses, the collapse load can be directly determined through optimization problems, offering a streamlined approach and reducing computational costs. In recent years, the application of second-order cone programming (SOCP) as an efficient optimization tool has gained prominence in various studies, leading to significant contributions in the field [1–5]. Simultaneously, multiple numerical procedures for limit and shakedown analyses, based on finite element methods and mathematical programming, have been developed over the past decades [6–11]. These endeavors aim to create a numerical tool that is efficient and robust enough for practical engineering applications.

In the realm of finite element framework, Liu et al. [12–14] introduced smoothed finite element methods (SFEM), wherein compatible strains are replaced by smoothed strains within local smoothing domains. Various types of SFEM,

such as cell-based SFEM (CS-FEM), node-based SFEM (NSFEM), edge-based (ES-FEM), and face-based SFEM (FS-FEM), exhibit distinct characters and properties, successfully applied in limit and shakedown analyses [5,15–17]. Among these models, the ES-FEM stands out for its effective properties in solving limit and shakedown analyses [18, 19]. Building on this research, the paper further develops ES-FEM for shakedown analysis of structures made of elastic-perfectly plastic material. The integration of ES-FEM with second-order cone programming in the shakedown static formulation ensures an effective and accurate solution to the optimization problem, minimizing computational efforts.

The paper adheres to the following organizational structure. The subsequent section introduces the static shakedown formulation in Section 2. . Section 3. provides a concise overview of the ES-FEM. Following this, Section 4. presents the formulation of the discretized problem as a second-order cone programming. To showcase the effectiveness of the proposed procedure, Section 5. includes a presentation of benchmark examples.

2. Static shakedown analysis

Consider an elastic-perfectly plastic structure subjected to a time-independent external load q. The structure is confined within a planar area Ω delineated by the static boundary Ω_t and the kinematic boundary Ω_u. A statically admissible stress field is approximated. The total stress at any point $\mathbf{x}$ within Ω is expressed as follows:

$$\boldsymbol{\sigma}(\mathbf{x},t) = \boldsymbol{\sigma}^{E}(\mathbf{x},t) + \boldsymbol{\rho}(\mathbf{x},t) \tag{1}$$

where $\boldsymbol{\sigma}^{E}$ and $\boldsymbol{\rho}$ denote the fictitious elastic stress and the residual stress, respectively. The obtained stress field is required to satisfy the equilibrium condition as well as the static boundary constraints for the static formulation. As the fictitious elastic stress field maintains equilibrium with the external pressure, the residual stress field is compelled to self-equilibrate.

Melnan's theorem states that shakedown behavior will occur when there exists a positive load multiplier λ and a residual stress field $\boldsymbol{\rho}$ that satisfies the yield function at any point of the structure for any loading path within the loading domain $\mathcal{P}$ at any time

$$\psi\left[\lambda\boldsymbol{\sigma}^{E}(\mathbf{x},t) + \boldsymbol{\rho}(\mathbf{x},t)\right] \leq 0, \ \forall \mathbf{x} \in \Omega \tag{2}$$

Following the work of König and Kleiber [20], shakedown behavior only occurs when the load paths reach the vertices of the convex load domain. Therefore, instead of checking the yield condition at all times of the loading cycle, it is sufficient to check at every vertex. The stress state at point $\mathbf{x}$ can be rewritten as follows:

$$\boldsymbol{\sigma}(\mathbf{x}) = \boldsymbol{\sigma}^{E}(\mathbf{x}) + \boldsymbol{\rho}(\mathbf{x}), \ \forall \mathbf{x} \in \Omega \tag{3}$$

The static principle of shakedown analysis can be now expressed as

$$\begin{aligned} \bar{\lambda}_{\mathrm{sd}} &= \max \lambda \\ &\text{s.t} \begin{cases} \nabla\boldsymbol{\rho}(\mathbf{x}) = 0, & \text{in } \Omega \\ \mathbf{n}\boldsymbol{\rho}(\mathbf{x}) = 0, & \text{on } \Gamma_t \\ \psi_{ik}\left[\lambda\boldsymbol{\sigma}^{E}(\mathbf{x}) + \boldsymbol{\rho}(\mathbf{x}), \sigma_p\right] \leq 0, & \text{in } \Omega \end{cases} \end{aligned} \tag{4}$$

where ψ_{ik} is the yield function corresponding to the i^{th} yield point and the k^{th} load vertex. The von Mises yield criterion is utilized in this study and is given for plane stress by

$$\psi_{ik}(\boldsymbol{\sigma}) = \sqrt{\sigma_{xx}^2 + \sigma_{yy}^2 + \sigma_{xx}\sigma_{yy} + 3\sigma_{xy}^2} - \sigma_p \tag{5}$$

and for plane strain by

$$\psi_{ik}(\boldsymbol{\sigma}) = \sqrt{\frac{1}{4}\left(\sigma_{xx} - \sigma_{yy}\right)^2 + \sigma_{xy}} - \sigma_p \tag{6}$$

where σ_{xx}, σ_{yy} and σ_{xy} respectively denote the nodal stress components, and σ_p is the yield stress of material. The outward surface normal is given as

$$\mathbf{n} = \begin{bmatrix} n_x & 0 \\ 0 & n_y \\ n_y & n_x \end{bmatrix} \tag{7}$$

It is worth noting that limit analysis is a special case of shakedown analysis when there is only one load, and it does not vary. The formulation (4) is then reduced to limit analysis.

3. Brief of ES-FEM

The computational domain is discretized into triangular elements. The smoothing domains associated with the edges are created by connecting the two end-points of the edge with the central point of adjacent elements, as illustrated in Figure 1.

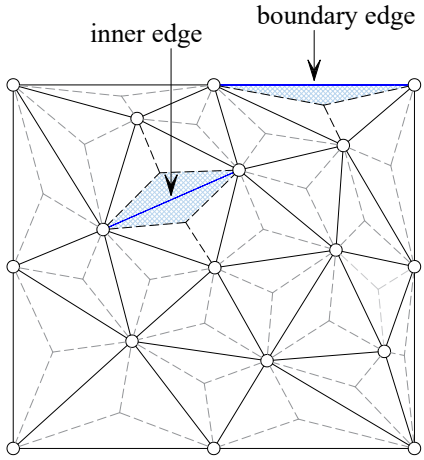

Fig. 1: Smoothing domains in ES-FEM.

Applying the strain smoothing technique as presented in [21], the smoothing version of the strain-displacement matrix can be assembled as follows:

$$\widetilde{\mathbf{B}}_I(\mathbf{x}_l) = \frac{1}{A_l^s}\sum_{j=1}^{\mathcal{N}_l^e}\frac{1}{3}A_j^e\mathbf{B}_j^e \tag{8}$$

where $\mathcal{N}_l^e$, A_j^e, and $\mathbf{B}_j^e$ denote the number of elements, area of the j^{th} element, and the compatible strain-displacement matrix of the j^{th} element around the considered edge l^{th}, respectively. The area of the smoothing domain A_l^s can be computed as:

$$A_l^s = \int_{\Omega_l^s}\mathrm{d}\Omega = \frac{1}{3}\sum_{j=1}^{\mathcal{N}_l^e}A_j^e \tag{9}$$

The matrix $\widetilde{\mathbf{B}}_I(\mathbf{x}_l)$ can be expressed as:

$$\widetilde{\mathbf{B}}_I = \begin{bmatrix} \widetilde{N}_{1,x} & 0 & \dots & \widetilde{N}_{\mathcal{N},x} & 0 \\ 0 & \widetilde{N}_{1,y} & \dots & 0 & \widetilde{N}_{\mathcal{N},y} \\ \widetilde{N}_{1,y} & \widetilde{N}_{1,x} & \dots & \widetilde{N}_{\mathcal{N},y} & \widetilde{N}_{\mathcal{N},x} \end{bmatrix} \tag{10}$$

where $\widetilde{N}_{I,x}$ and $\widetilde{N}_{I,y}$ denote the smoothed shape function derivatives.

4. Numerical discretization

Introduce the additional variable vector $\mathbf{r} = [r_1, r_2, r_3, r_4]^{\mathrm{T}}$ for plane stress as follows:

$$r_1 = \sigma_p \tag{11}$$

$$r_{2\to4} = \mathbf{J}^{\mathrm{T}}\boldsymbol{\sigma} = \mathbf{J}^{\mathrm{T}}(\lambda\boldsymbol{\sigma}^E + \boldsymbol{\rho}) \tag{12}$$

where

$$\mathbf{J} = \frac{1}{2}\begin{bmatrix} 2 & 0 & 0 \\ -1 & \sqrt{3} & 0 \\ 0 & 0 & 2\sqrt{3} \end{bmatrix} \tag{13}$$

Similarly, the vector consisting of additional variables for plane strain is given by

$$\mathbf{r} = \begin{bmatrix} r_1 \\ r_2 \\ r_3 \end{bmatrix} = \begin{bmatrix} \sigma_p \\ \frac{1}{2}(\sigma_{xx} - \sigma_{yy}) \\ \sigma_{xy} \end{bmatrix} \tag{14}$$

Hence, the von Mises failure criterion can be rewritten in the standard form of SOCP for the plane stress problem as

$$\mathcal{L} = \left\{\mathbf{r} \in \mathrm{R}^3 \mid r_1 \geq \| r_{2\to4} \|_{L^2}\right\} \tag{15}$$

and for plane strain as

$$\mathcal{L} = \left\{\mathbf{r} \in \mathrm{R}^3 \mid r_1 \geq \| r_{2\to3} \|_{L^2}\right\} \tag{16}$$

The static formulation of shakedown analysis in Equation (4) is now formulated as an SOCP optimization problem as follows:

$$\begin{aligned} &\bar{\lambda}_{\mathrm{sd}} = \max \lambda \\ &\text{s.t} \begin{cases} \nabla\boldsymbol{\rho} = 0, & \text{in } \Omega \\ \mathbf{n}\boldsymbol{\rho} = 0, & \text{on } \Gamma_t \\ \mathbf{r}_{ik} \in \mathcal{L}_{ik}, & \text{in } \Omega \end{cases} \end{aligned} \tag{17}$$

The equivalent weak form of the equilibrium condition and static boundary condition in Equation (17) can be expressed as

$$\int_\Omega \delta\boldsymbol{\epsilon}^{\mathrm{T}}\boldsymbol{\rho}\,\mathrm{d}\Omega = 0 \tag{18}$$

where $\delta\boldsymbol{\epsilon}$ denotes the virtual strain approximated based on the fictitious displacement field using the relation $\delta\epsilon_{ij} = (\delta u_{i,j} + \delta u_{j,i})$ as

$$\delta\boldsymbol{\epsilon} = \widetilde{\mathbf{B}}\delta\mathbf{u} \tag{19}$$

where the strain-displacement matrix $\widetilde{\mathbf{B}}$ is defined as Equation (8). The weak form in Equation (18) can now be expressed as

$$\int_{\Omega} \left(\widetilde{\mathbf{B}}\delta\mathbf{u}\right)^{\mathrm{T}} \boldsymbol{\rho}\, \mathrm{d}\Omega = (\delta\mathbf{u})^{\mathrm{T}} \int_{\Omega} \widetilde{\mathbf{B}}^{\mathrm{T}} \boldsymbol{\rho}\, \mathrm{d}\Omega = 0 \quad (20)$$

Due to $\delta\mathbf{u}$ being arbitrary, by using nodal integration, the above constraints can be satisfied if

$$\begin{aligned} \int_{\Omega} \widetilde{\mathbf{B}}^{\mathrm{T}} \boldsymbol{\rho}\, \mathrm{d}\Omega &= \sum_{k=1}^{\mathcal{N}_v} \sum_{i=1}^{\mathcal{N}} \widetilde{\mathbf{B}}^{\mathrm{T}} A_i \boldsymbol{\rho}_{ik} \\ &= \sum_{k=1}^{\mathcal{N}_v} \sum_{i=1}^{\mathcal{N}} \mathbf{C}_{ik} \boldsymbol{\rho}_{ik} = 0 \end{aligned} \quad (21)$$

where $\mathcal{N}$ is the number of yield points, $\mathcal{N}_v$ is the number of load vertices, A_i denotes the area of the smoothing domain i^{th}, and $\mathbf{C}$ is the matrix that embodies the equilibrium conditions and static boundary conditions.

Finally, the optimization problem is presented in the following formulation:

$$\begin{aligned} &\bar{\lambda}_{\mathrm{sd}} = \max \lambda \\ &\text{s.t} \begin{cases} \sum_{k=1}^{\mathcal{N}_v} \sum_{i=1}^{\mathcal{N}} \mathbf{C}_{ik} \boldsymbol{\rho}_{ik} = 0 \\ \mathbf{r}_{ik} \in \mathcal{L}_{ik} \end{cases} \end{aligned} \quad (22)$$

It is important to note that the constraints in Equation (22), which include the equilibrium condition, the boundary condition, as well as the yield criterion, are not precisely satisfied at every point in the computational domain. Additionally, the fictitious elastic stress field is an approximation of the exact field. Therefore, the multiplier $\bar{\lambda}$ obtained by Equation (22) represents only a quasi-lower-bound solution. However, with a sufficiently fine discretization of the problem domain, the proposed approach can be guaranteed to provide an accurate and reliable value for $\bar{\lambda}$.

5. Numerical results

5.1. Thin plate with a circular cutout at center

The first investigation involves a thin square plate with a central circular cutout under biaxial pressure, as depicted in Figure 2(a). The provided data includes Young's modulus $E = 2.1 \times 10^5$ MPa, Poisson's ratio $\nu = 0.3$, and the material's yield stress $\sigma_p = 200$ MPa. The ratio of the plate's length to the hole's diameter is 5. Since geometric and loading symmetry, only the upper-right quarter of the plate is considered, as shown in Figure 2(b). Figure 2(c) illustrates the numerical discretization of the problem domain using 176 triangular elements.

Tab. 1: Plate hole ($p_1 \neq 0$, $p_2 = 0$): computed collapse load factors.

$\mathcal{N}_e$	FEM-T3		ESFEM-T3		
	λ_{lm}	e (%)	λ_{lm}	e (%)	τ (s)
130	0.8184	2.29	0.8120	1.50	0.01
414	0.8066	0.82	0.8041	0.51	0.03
1008	0.8029	0.37	0.8018	0.23	0.06
1656	0.8019	0.23	0.8012	0.15	0.09
2508	0.8013	0.16	0.8008	0.10	0.12
3484	0.8009	0.11	0.8006	0.07	0.24

$\mathcal{N}_e$: number of elements, e (%): relative error, τ (s): optimization time.

Tab. 2: Plate hole: comparison of solutions (λ_{lm})

Author	Load cases (p_1, p_2)		
	(1, 0)	(1, 0.5)	(1, 1)
Present study	0.8006	0.911	0.896
Le *et al.* [17]	0.8010	0.911	0.895
Chen *et al.* [22]	0.7980	0.899	0.874
Zouain *et al.* [6]	0.8030	0.911	0.894
Groβ-Weege [23]	0.7920	0.891	0.882
Ho *et al.* [16]	0.8007	0.911	0.896
Ho and Le [11]	0.8001	0.902	0.871

The collapse and shakedown limits corresponding to various loading conditions are consolidated in Tables 1, 2, and 3. In the limit analysis case with the load ($p_1 \neq 0$, $p_2 = 0$), Gaydon and McCrum [25] reported an analytical solution of 0.800. This study addresses the problem using FEM-T3 and ES-FEM-T3 models for comparison purposes. The obtained load factors are 0.8009 and 0.8006, with relative errors

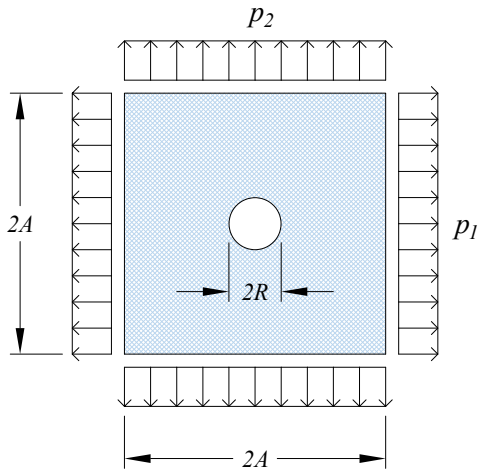

(a) Geometry, dimensions, and loading

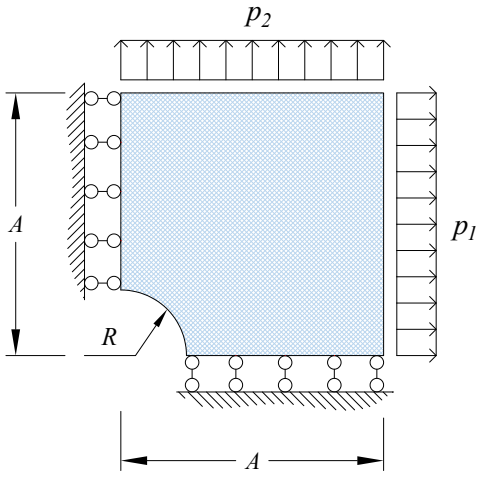

(b) Computational domain

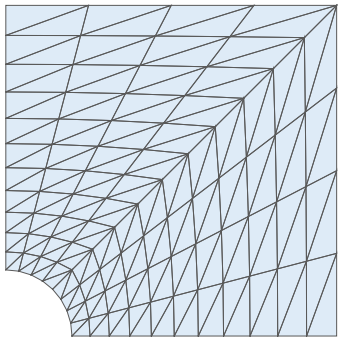

(c) Finite element discretization

Fig. 2: Plate hole problem.

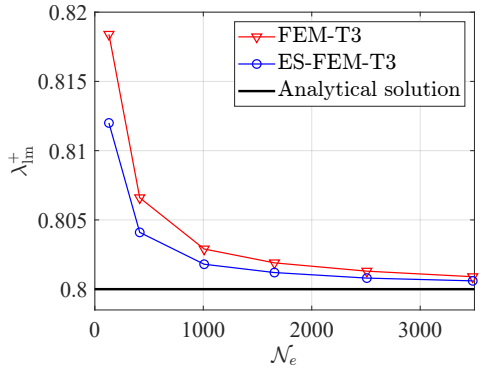

(a) Collapse load factors

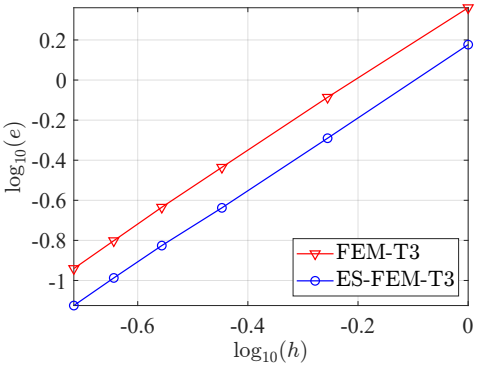

(b) Convergence rate

Fig. 3: Plate hole ($p_1 \neq 0$, $p_2 = 0$): computed collapse load multipliers and convergence analysis.

Tab. 3: Plate hole: comparison of solutions (λ_{sd})

Author	Load cases (p_1, p_2)		
	(1, 0)	(1, 0.5)	(1, 1)
Present study	0.623	0.525	0.424
Zouain *et al.* [6]	0.594	0.500	0.429
Groβ-Weege [23]	0.614	0.524	0.446
Ho *et al.* [16]	0.617	0.536	0.449
Ho and Le [11]	0.650	0.551	0.478
Genna [24]	0.604	0.508	0.438
Tran *et al.* [18]	0.610	0.514	0.444

compared to [25] being 0.11% and 0.07%, respectively. Graphs 3(a) and 3(b) present the convergence analysis of obtained solutions, demonstrating that the proposed methods align well with the analytical procedure. Notably, the results indicate that ES-FEM-T3 outperforms FEM-T3.

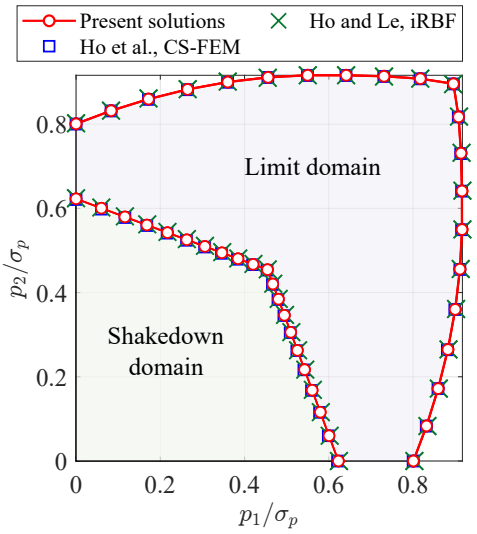

Fig. 4: Plate hole: interaction diagrams.

As previously noted, this formulation does not guarantee strictly bounding characteristics, and numerical results obtained by the static formulation can be higher than the analytical ones. However, considering the relative errors between these results and those in [25], all of them are less than 1%, demonstrating the accuracy and reliability of the proposed approach.

The time consumption, as observed in Table 1, illustrates that the utilization of second-order cone programming in this study enables the rapid solution of optimization problems with thousands of variables, typically in less than 1 second. This showcases the potential to expand the proposed method to large-scale practical engineering problems.

Figure 4 shows the loading domains of both limit and shakedown cases, which are also compared with previous authors. The comparisons in Tables 2 and 3 demonstrate the validity and reasonability of the current method.

5.2. Simple frame

This section examines a simple frame with two different boundary conditions. In the first case, only the vertical displacement on the left boundary is constrained, while in the second model, both the horizontal and vertical displacements are constrained. Figure 5(a) illustrates the dimensions, boundary conditions, and loading. The input data includes $E = 2 \times 10^5$ MPa, $\nu = 0.3$, $\sigma_p = 10$ MPa, and a frame thickness of $t = 10$cm. The frame is subjected to a biaxial variable load, satisfying $0.4 \leq p_1 \leq 1$ and $1.2 \leq p_2 \leq 3$. The discretization is depicted in Figure 5(b).

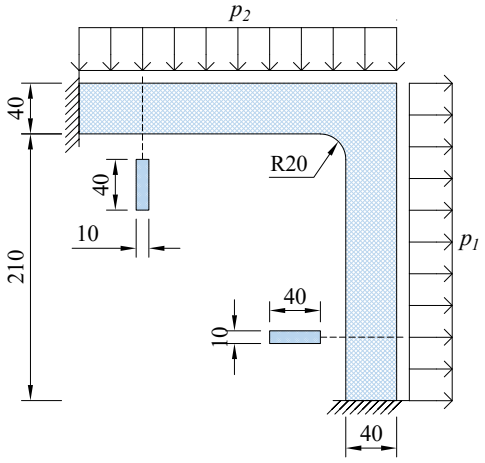

(a) Geometry, dimensions, and loading

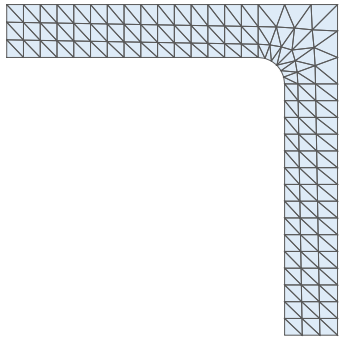

(b) Finite element discretization

Fig. 5: Simple frame problem.

This problem was initially investigated by Garcea et al. [26], and subsequent examinations were conducted by Ho et al. [11, 16]. The comparison between the present solutions using ES-FEM-T3 and the results in [11, 16, 26], as shown in Tables 4 and 5, serves as a reliability assessment for the proposed method.

Tab. 4: Simple frame: comparison of solutions (λ_{lm})

Case 1	(p_1, p_2)		
	(0.4, 3)	(1, 1.2)	(1, 3)
Present study	2.994	2.836	2.653
Garcea *et al.* [26]	2.831	2.975	2.645
Ho *et al.* [16]	2.981	2.820	2.634
Ho and Le [11]	3.153	2.979	2.728
Case 2	(p_1, p_2)		
	(0.4, 3)	(1, 1.2)	(1, 3)
Present study	4.204	7.854	3.945
Garcea *et al.* [26]	4.207	7.804	3.949
Ho *et al.* [16]	4.186	7.810	3.931
Ho and Le [11]	4.152	8.095	3.874

Tab. 5: Simple frame ($0.4 \leq p_1 \leq 1$ and $1.2 \leq p_2 \leq 3$): comparison of solutions (λ_{sd})

Author	Case 1	Case 2
Present study	2.473	3.918
Garcea *et al.* [26]	2.473	3.925
Ho *et al.* [16]	2.452	3.817
Ho and Le [11]	2.649	3.964

5.3. Symmetric continuous beam

This example investigates a symmetric continuous beam undergoing a loading combination $(p_1,\ p_2)$, where each single load varies independently, such that $1.2 \leq p_1 \leq 2$ and $0 \leq p_2 \leq 1$, as depicted in Figure 6(a). The material properties are provided as $E = 1.8 \times 10^5$ MPa, $\nu = 0.3$, $\sigma_p = 100$ MPa. Figure 6(b) illustrates the finite element discretization.

Various loading scenarios are examined, and the corresponding limit and shakedown load multipliers are presented in Table 6. The problem has been investigated using different numerical approaches with various optimization algorithms found in the literature [11,16,22,26]. The comparison shown in Table 6 implies that the present solutions align well with the published results in previous papers.

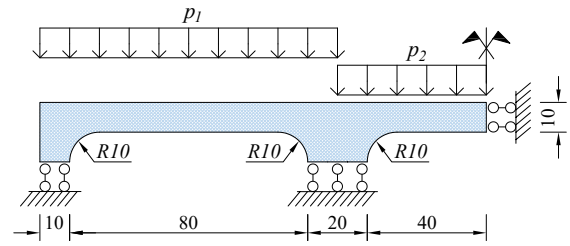

(a) Geometry, dimensions, and loading

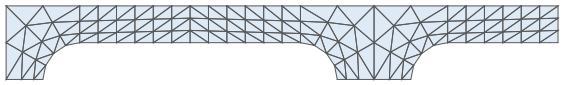

(b) Finite element discretization

Fig. 6: Continuous beam problem.

5.4. Grooved plate

The last example involves a grooved plate subjected to a combination of a traction force p_N and a bending load p_M, as depicted in Figure 7(a), where $R = 250$mm, and $L = 4R$. The numerical discretization using triangular elements is illustrated in Figure7(b). The load domain is specified as $0 \leq p_N \leq \sigma_p$ and $0 \leq p_M \leq \sigma_p$. The input data include $E = 2.1 \times 10^5$ MPa, $\nu = 0.3$, and $\sigma_p = 116.2$ MPa.

Two loading scenarios are examined, including pure tension ($p_M = 0$, $p_N \neq 0$) and tension combined with bending ($p_M \neq 0$, $p_N \neq 0$). The plane stress condition is taken into account for this problem. Table 7 compares the limit and shakedown load multipliers with those obtained from other approaches. It is observed that the numerical solutions provided by the proposed approach align well with the available results in the literature.

6. Conclusions

An equilibrium edge-based finite element formulation has been successfully applied to the shakedown analysis of structures. Implementing a smoothing technique ensures that only one integration point is required for each smoothing domain, minimizing the size of the resultant problem. The optimization problem is formulated as conic programming and efficiently solved using

Tab. 6: Continuous beam: comparison of solutions

	λ_{lm}				λ_{sd}		
(p_1, p_2)	(2, 0)	(0, 1)	(1.2, 1)	(2, 1)	$p_1 \in [1.2, 2]$ $p_2 \in [0, 1]$	$p_1 \in [0, 2]$ $p_2 \in [0.6, 1]$	$p_1 \in [0, 2]$ $p_2 \in [0, 1]$
Present study	3.290	8.728	5.486	3.291	3.249	2.160	2.142
Garcea *et al.* [26]	3.280	8.718	5.467	3.280	3.244	-	-
Chen *et al.* [22]	-	-	-	-	3.297	2.174	2.152
Ho *et al.* [16]	3.301	8.748	5.504	3.302	3.362	2.228	2.205
Ho and Le [11]	3.225	8.836	5.530	3.309	3.217	2.333	2.308

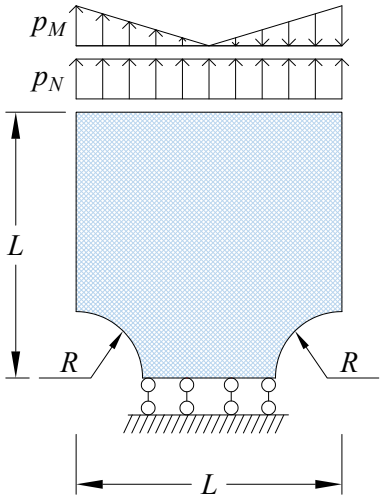

(a) Computational domain

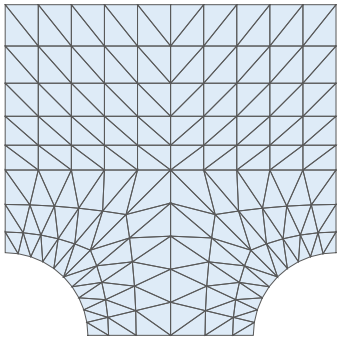

(b) Discretization

Fig. 7: Grooved plate problem.

Tab. 7: Grooved plate: comparisons of solutions.

λ_{lm}	$p_M = 0$ $p_N \neq 0$	$pM \neq 0$ $p_N \neq 0$
Present study	0.557	0.28867
Tran *et al.* [18]	0.562	0.27811
Nguyen-Xuan *et al.* [15]	0.559	0.29660
Ho *et al.* [16]	0.557	0.29394
Ho and Le [11]	0.524	0.25832
Vu [27]	0.557	-
Casciaro and Cascini [28]	0.568	-
Prager and Hodge [29]	0.500	-
Yan [30], numerical	0.558	-
Yan [30], analytical	0.5 - 0.577	-
λ_{sd}	$0 \leq p_M \leq \sigma_p$ $0 \leq p_N \leq \sigma_p$	
Present study	0.23916	
Tran *et al.* [18]	0.23603	
Nguyen-Xuan *et al.* [15]	0.22477	
Ho *et al.* [16]	0.24807	
Ho and Le [11]	0.22024	
Vu [27]	0.23494	

advanced tools, reducing computational costs. Comparative analysis of the obtained results demonstrates robust concordance with numerical models derived from previous studies within the existing literature.

In this study, the shakedown formulation is grounded in the elastic-perfectly plastic material model. For future investigations, it is advisable to expand the study by incorporating the material's hardening state. This expansion would enable a more precise simulation of the structure's realistic behavior and a more effective utilization of the material's bearing capacity. Additionally, at the limit state, plastic zones, as indi-

cated by the plastic dissipation power or stress field, are predominantly localized within small regions within the computational domain. Consequently, adaptive mesh refinement, which concentrates on refining the mesh in plastic regions while maintaining a coarser mesh elsewhere, can be applied to enhance computational efficiency.

References

[1] K. Krabbenhoft, A.V. Lyamin, and S.W. Sloan. Formulation and solution of some plasticity problems as conic programs. *Int. J. Solids Struct.*, 44(5):1533–1549, 2007.

[2] A. Makrodimopoulos. Remarks on some properties of conic yield restrictions in limit analysis. *Int. J. for Numer. Methods Biomed. Eng.*, 26(11):1449–1461, 2010.

[3] C.V. Le, M. Gilbert, and H. Askes. Limit analysis of plates and slabs using a meshless equilibrium formulation. *Int. J. for Numer. Methods Eng.*, 83(13):1739–1758, 2010.

[4] C.V. Le, H. Askes, and M. Gilbert. Adaptive element-free galerkin method applied to the limit analysis of plates. *Comput. Methods Appl. Mech. Eng.*, 199(37-40):2487–2496, 2010.

[5] C.V Le, H. Nguyen-Xuan, H. Askes, T. Rabczuk, and T. Nguyen-Thoi. Computation of limit load using edge-based smoothed finite element method and second-order cone programming. *Int. J. Comput. Methods*, 10(01):1340004, 2013.

[6] N. Zouain, L. Borges, and J.L. Silveira. An algorithm for shakedown analysis with nonlinear yield functions. *Comput. Methods Appl. Mech. Eng.*, 191(23-24):2463–2481, 2002.

[7] H. Magoariec, S. Bourgeois, and O. Debordes. Elastic plastic shakedown of 3D periodic heterogeneous media: a direct numerical approach. *Int. J. Plast.*, 20(8):1655–1675, 2004.

[8] V.D. Khoi, A.M. Yan, and H. Nguyen-Dang. A dual form for discretized kinematic formulation in shakedown analysis. *Int. J. Solids Struct.*, 41(1):267–277, 2004.

[9] Y.H. Liu, X.F. Zhang, and Z.Z. Cen. Lower bound shakedown analysis by the symmetric galerkin boundary element method. *Int. J. Plast.*, 21(1):21–42, 2005.

[10] G. Garcea, G. Armentano, S. Petrolo, and R. Casciaro. Finite element shakedown analysis of two-dimensional structures. *Int. J. for Numer. Methods Eng.*, 63(8):1174–1202, 2005.

[11] P.L.H. Ho and C.V. Le. A stabilized irbf mesh-free method for quasi-lower bound shakedown analysis of structures. *Comput. & Struct.*, 228:106157, 2020.

[12] G. R. Liu, T.T Nguyen, K.Y. Dai, and K.Y. Lam. Theoretical aspects of the smoothed finite element method (SFEM). *Int. J. for Numer. Methods Eng.*, 71(8):902–930, 2007.

[13] H. Nguyen-Xuan, S. Bordas, and H. Nguyen-Dang. Smooth finite element methods: Convergence, accuracy and properties. *Int. J. for Numer. Methods Eng.*, 74(2):175–208, 2008.

[14] G. R. Liu, T. Nguyen-Thoi, H. Nguyen-Xuan, K.Y. Dai, and K.Y. Lam. On the essence and the evaluation of the shape functions for the smoothed finite element method (sfem). *Int. J. for Numer. Methods Eng.*, 77(13):1863–1869, 2009.

[15] H. Nguyen-Xuan, T. Rabczuk, T. Nguyen-Thoi, T.N. Tran, and N. Nguyen-Thanh. Computation of limit and shakedown loads using a node-based smoothed finite element method. *Int. journal for numerical methods engineering*, 90(3):287–310, 2012.

[16] P.L.H. Ho, C.V. Le, and T.Q. Chu. The equilibrium cell-based smooth finite element method for shakedown analysis of structuresn. *Int. J. Comput. Methods*, 16(05):1840013, 2019.

[17] C.V. Le, H. Nguyen-Xuan, H. Askes, S. Bordas, T. Rabczuk, and H. Nguyen-Vinh. A cell-based smoothed finite element method for kinematic limit analysis. *Int.*

J. for Numer. Methods Eng., 83(12):1651–1674, 2010.

[18] T.N. Tran, G.R. Liu, H. Nguyen-Xuan, and T. Nguyen-Thoi. An edge-based smoothed finite element method for primal–dual shakedown analysis of structures. *Int. J. for Numer. Methods Eng.*, 82(7):917–938, 2010.

[19] C.V. Le, H. Nguyen-Xuan, H. Askes, T. Rabczuk, and T. Nguyen-Thoi. Computation of limit load using edge-based smoothed finite element method and second-order cone programming. *Int. J. Comput. Methods*, 10(01):1340004, 2013.

[20] J.A. Konig and M. Kleiber. On a new method of shakedown analysis. *Bull. de Acad. Polonaise des Sci. des Sci. Tech.*, 4:165–171, 1978.

[21] J.S. Chen, C.T. Wu, S. Yoon, and Y. You. A stabilized conforming nodal integration for galerkin mesh-free methods. *Int. journal for numerical methods engineering*, 50(2):435–466, 2001.

[22] S. Chen, Y. Liu, and Z. Cen. Lower-bound limit analysis by using the EFG method and non-linear programming. *Int. J. for Numer. Methods Eng.*, 74(3):391–415, 2008.

[23] J. Groβ-Weege. On the numerical assessment of the safety factor of elastic-plastic structures under variable loading. *Int. J. Mech. Sci.*, 39(4):417–433, 1997.

[24] F. Genna. A nonlinear inequality, finite element approach to the direct computation of shakedown load safety factors. *Int. journal mechanical sciences*, 30(10):769–789, 1988.

[25] F.A. Gaydon and A.W. McCrum. A theoretical investigation of the yield point loading of a square plate with a central circular hole. *J. Mech. Phys. Solids*, 2(3):156–169, 1954.

[26] G. Garcea, G. Armentano, S. Petrolo, and R. Casciaro. Finite element shakedown analysis of two-dimensional structures. *Int. journal for numerical methods engineering*, 63(8):1174–1202, 2005.

[27] D.K. Vu. *Dual limit and shakedown analysis of structures*. PhD thesis, Doctor thesis, University of Liege Faculty of Applied Sciences, Liege, 2001.

[28] R. Casciaro and L. Cascini. A mixed formulation and mixed finite elements for limit analysis. *Int. J. for Numer. Methods Eng.*, 18(2):211–243, 1982.

[29] W. Prager and P.G. Hodge. Theory of perfectly plastic solids. *John Wiley & Sons*, 1951.

[30] A.M. Yan. *Contributions to the direct limit state analysis of plastified and cracked structures*. PhD thesis, Universite de Liege, Faculte des Sciences appliquees, 1999.

About Authors

Phuc L. H. HO graduated with a Bachelor's degree in Civil Engineering from Ho Chi Minh City University of Technology, Vietnam, in 2011, and subsequently completed his Master's degree in 2013. He earned his Ph.D. in Engineering Mechanics from Ho Chi Minh City University of Technology and Education, Vietnam, in 2021. Currently, he serves as a research professor at Dong-A University, Busan, South Korea, affiliated with the University Core Research Center for Disaster-free and Safe Ocean City Construction (D-SOC). His research specialization includes the analysis of structures and materials under limit states using advanced computational methods, focusing primarily on fundamental structural elements and geotechnical issues.

Dung T. TRAN receiced his B.S degree in Building Material Engineering from Ho Chi Minh City University of Technology, Vietnam in 2005 and M.S degree in Mechanics of Constructions from University of Liège, Belgium in 2007. He earned his Ph.D. in Mechanics of Solid Object from University of Science, Viet Nam National University Ho Chi Minh City, Vietnam in 2018. He is currently a lecturer at the Civil Engineering, Ho Chi Minh City Open University, Vietnam. His research interests include numerical methods, limit analysis and shakedown of structures.